KAWASAKI STEEL TECHNICAL REPORT
No.13 (September 1985)

Fe-36% Ni Invar Type Alloy KLN 36 for LNG Facilities

Kiyohiko Nohara, Akio Ejima

Synopsis :
Since Fe-36%Ni steel (Inver type alloy) exhibits low thermal expansively, it has been used as the membrane material for LNG facilities. However, there is a drawback of so high susceptibility to hot cracking during welding due to its complete austenitic structure. As a result of study on the influence of chemical compositions of various elements and some conditions in manufacturing processes, it is made clear that both lowering of impurity elements and addition of tantalum can markedly improve the resistance to hot cracking during welding. This is in accordance with the result of a thermal cycle simulation experiment. The study is also made on physical properties including thermal expansively and mechanical properties of this improved steel (KSC's low thermal expansion alloy: KLN 36) to show that it is totally furnished with assorted characteristics as the LNG material.

The body can be viewed from the next page.

Fe-36% Ni Invar Type Alloy KLN 36 for LNG Facilities*

Kiyohiko Nohara
Dr. Engi., Senior Researcher, New Materials Research Center, High-Technology Research Labs.

Akio Ejima
Assistant Director, I & S Research Labs.

Synopsis:

Since Fe-36%Ni steel (Invar type alloy) exhibits low thermal expansivity, it has been used as the membrane material for LNG facilities. However, there is a drawback of so high susceptibility to hot cracking during welding due to its complete austenitic structure. As a result of study on the influence of chemical compositions of various elements and some conditions in manufacturing processes, it is made clear that both lowering of impurity elements and addition of tantalum can markedly improve the resistance to hot cracking during welding. This is in accordance with the result of a thermal cycle simulation experiment. The study is also made on physical properties including thermal expansivity and mechanical properties of this improved steel (KSC's low thermal expansion alloy: **KLN 36***) to show that it is totally furnished with assorted characteristics as the LNG material.*

1 Introduction

Fe-36%Ni steel (Invar type alloy) has its thermal expansivity about 1/10 that of stainless steel or aluminum alloys at temperatures ranging from the boiling point of LNG (liquefied natural gas, about −162°C) to room temperature.[1] Since this steel is composed of a single austenitic structure which is stable at low temperatures, it has excellent ductility and toughness, is free of embrittlement, and shows stable cryogenic mechanical properties. It also has low notch susceptibility. Consequently, it is frequently used as cryogenic membrane material in tanks of LNG carriers and on-shore LNG facilities.[2]

A problem with this steel, however, is its high sensitivity to hot cracking during welding, which is related to its complete austenitic phase. A source of concern is that the steel will develop hot cracking when automatic or manual welding is performed in the construction of LNG tanks, or when welding repairs are conducted. Weld cracking is related to welding methods and conditions,[3] but in this paper, the possibility of improvement of the weld cracking resistance of the material itself is examined in terms of the chemical composition balance and manufacturing conditions of the material.

Further, at the construction of tanks the anti-rust property of this steel also poses a problem. To cope with this problem, air-conditioning and surface treatment of steel plates have been considered,[4] but here, improvement in the anti-rust property through composition adjustment and the effects of additive elements are examined.

As mentioned above, studies were made on resistance to hot cracking during welding, the anti-rust property, and composition balance. An improved Fe-36%Ni steel (Kawasaki low thermal expansivity alloy for cryogenic services: **KLN 36**), which was developed as a result of such studies, was investigated with respect to physical properties, such as thermal expansivity, and mechanical properties, including formability. Further, it was used in construction of a model tank as a means of examining its applicability as membrane material for LNG facilities.

2 Test Method

2.1 Test Material

The effects of the basic composition and impurity ele-

* Originally published in *Kawasaki Steel Giho*, 17(1985)2, 169-177

Table 1 Chemical composition range of specimens (wt%)

Basic elements					Impurity elements				Additional elements			
C	Si	Mn	Ni	Al	P	S	O	N	Ta	Ti, Nb, V, Zr	Cr	Co
0.017 ~ 0.047	0.16 ~ 0.51	0.31 ~ 1.04	34.97 ~ 36.30	0.001 ~ 0.026	0.0005 ~ 0.012	0.0004 ~ 0.008	0.0012 ~ 0.0067	0.0007 ~ 0.0086	0.001 ~ 0.05	0.05	0.1 ~ 0.5	0.1 ~ 0.5

ments of this steel as well as of additive alloy elements on weld-cracking and anti-rust properties were studied. For this purpose, a group of specimens in which the contents of C, Si, Mn, Ni, Al, P, S, O, and N were varied and another group of specimens in which additive elements such as Cr, Co, Ta, Ti, Nb, V, and Zr were altered were vacuum-melted into small ingots, each weighing 50 kg, within the composition ranges shown in **Table 1**. The ingots were later slabbed and then hot-and cold-rolled into 10 mm thick steel plates and 1.5 mm sheets. In this case, a considerable number of edge crakcs occurred in specimens containing large amounts of impurity elements, and, in particular, with those high in S.

Further, a 5 ton ingot with a composition determined on the basis of the results of the small ingot experiment was produced by vacuum melting in an electro-magnetic induction furnace. It was then slabbed, hot and cold rolled, and finished by continuous bright annealing at commercial production facilities and processed into cold strip coils of 0.5, 1.0 and 1.5 mm thicknesses. These coils, as will be detailed below, were used in the construction of a trial model membrane tank of the type used in GT (Gaz Transport) LNG carriers, in order to examine formability, weldability, general fabricability, and operational performance.

2.2 Weld Cracking Test

As the principal weld cracking test, the cross-bead type varestraint crack test was performed. A surface-ground 10 mm thick specimen was given a first pass by TIG welding under an Ar gas shield. Next, a crack test specimen measuring 10 mm$t$ × 50 mm$W$ × 350 mm$L$ was taken and a second welding pass, also by TIG welding under an Ar gas shield, was laid on the specimen at 90° to the first pass. When the electrode reached the position where maximum strain was applied at the center of the first bead, the test specimen was bent rapidly in order to apply strain.

The cross-bead hot cracking tensile test [5-7] was also used. Steel sheet specimens, 1.5 mm thick, were TIG-welded in the same way as in actual tank construction. To obviate the effects of changes in oxygen and nitrogen contents in the weld, first-pass welding was performed in a chamber filled with pure argon gas. Next, a crack test specimen measuring 1.5 mm$t$ × 50 mm$W$ × 150 mm$L$ was taken. A second pass was laid on this specimen in a direction which crossed the first pass by TIG welding under an Ar gas shield. During welding, constant tensile load was applied to the specimen.

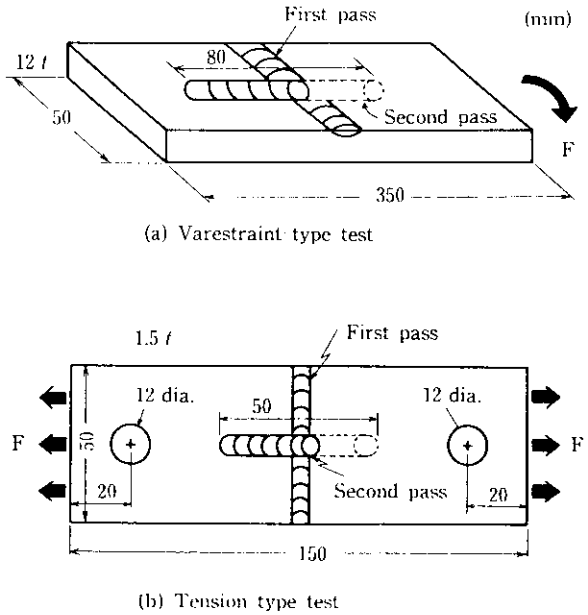

(a) Varestraint type test

(b) Tension type test

Fig. 1 Shapes and sizes of weld-cracking test specimens (a) varestraint-type test (b) tension type test

Table 2 TIG welding conditions for weld-cracking test

Test		Voltage (V)	Current (A)	Speed (mm/min)
Varestrain-type	1st pass	12	200	100
	2nd pass	10	150	100
Tension-type	1st pass	7	40	100
	2nd pass	11	60	100

Shapes and sizes of specimens for both the varestraint and tension tests and the welding conditions of various beads are shown in **Fig. 1** and **Table 2**, respectively. In both test methods, the number of cracks and the total length of cracks in the first bead were measured to judge

crack susceptibility. Further, optical microscopic observation and analyses by microanalyzer and macroanalyzer were made. A rapid heating and tension test was also conducted, using the Gleeble testing machine to examine the high temperature ductility of the specimen to determine its relation to weld cracking susceptibility.

2.3 Measurement of Physical and Mechanical Properties

Thermal expansion characteristics of the steel were measured by the horizontal thermal expansion measuring apparatus, in which temperature control was given in a liquefied nitrogen atmosphere, using a test specimen measuring 5 mmϕ and 50 mm$L$. The measured temperature range was −185 to 20°C, and the heating rate was 2°C/min. In addition, physical properties, such as Young's modulus, specific heat, electric resistance, density, thermal conductivity and the Curie point (magnetic transformation point) of steel of typical composition, were measured.

Mechanical properties were measured in a room-temperature and cryogenic (liquefied nitrogen temperature) tensile test, Charpy impact test, and fatigue and hardness tests. At the same time, a 0.2-mm-R V-notch tensile test was conducted. Shapes and sizes of specimens for mechanical tests and test methods conformed to the JIS specifications.

3 Test Results and Discussion

3.1 Welding Test

3.1.1 Weld cracking phenomenon

A typical example of cracking occurring in the cross-bead-type tensile weld cracking test is shown in **Photo 1**. In the preparation of the photo, the cross bead sample of a welded specimen was covered with resin, buff-ground, and given electrolytic etching with a 10% oxalic acid solution; it was found that cracks had generated on the first bead in a direction parallel to the bead. The cracked portions corresponded to the HAZ of the second bead. This indicates that, with Fe-36%Ni steel, the previous pass is susceptible to hot cracking during welding, due to the effect of heating in the succeeding pass. Therefore, in actual welding, it is feared that such cracks may occur during repairs involving welding. Conceivable causes of crack development include materials, welding conditions, and such constraining states as stress and strain.

As seen in Photo 1, this hot cracking during welding appears to have been generated at the solidification crystal boundary, but in fact it was generated on the moved γ grain boundary which was formed in the reheating process as shown in **Photo 2**. It is considered that this

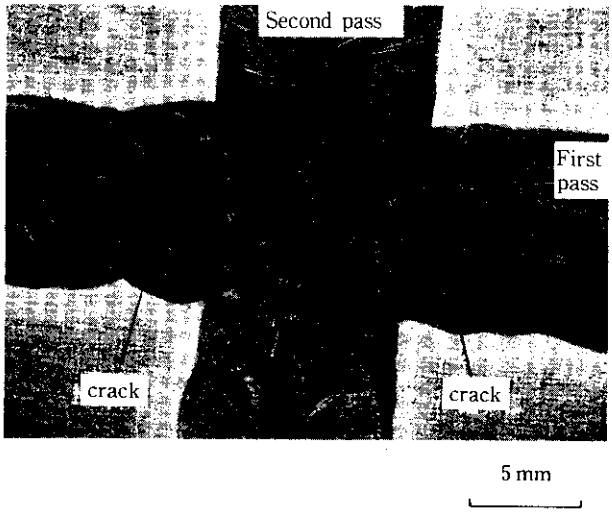

Photo 1 Macrophotograph of welded specimen

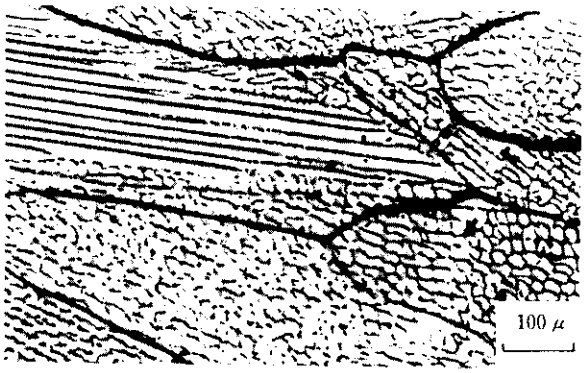

Photo 2 Micro hot cracks in welded cross bead

Photo 3 SEM image of fractured surface of hot cracking weld test specimen

moved γ grain boundary becomes embrittled during reheating and develops hot cracking when it is unable to withstand constraint stress. As shown in the scanning electron micrograph of the fracture surface of the crack in **Photo 3**, this cracking is a ductility-drop crack, and in some rare cases, liquefaction cracking is generated in

the vicinity of the fusion boundary.

3.1.2 Effects of impurity elements, basic composition, and manufacturing conditions

The authors conducted the weld cracking test mentioned in Sec. 2 to ascertain conditions which will decrease or obviate hot cracking during welding through control of material composition and manufacturing conditions, rather than through control of welding conditions or methods.

Since cracking in this steel can be attributed to a ductility-drop generated on the γ grain boundary, the authors first investigated the effects of impurity elements, P and S, which frequently cause grain boundary embrittlement of stable austenitic steel. **Figures 2** and **3** show the independent effects of P and S, respectively, in the varestraint-type test. It was feared that the hot cracks which occurred in the first bead in the reheating process might occur in actual welding work. And in this test method, cracks occurred on the second bead in the solidification process and thus both types of cracks, reheating and solidification, were counted. It was observed that (1) P and S cause cracking, even if their contents are as small as about 0.005%, (2) solidification cracking is more likely to occur than reheating cracking, if the contents of impurity elements are equal, and (3) S causes greater susceptibility to cracking than P. (With respect to (2), solidification cracking is less likely to occur in the constrained tension test, this difference being seemed attributable to differences in the states of stress and strain between the two test methods; in either of these test methods, the hot cracking phenomenon which may cause problems in actual welding work can be simulated.)

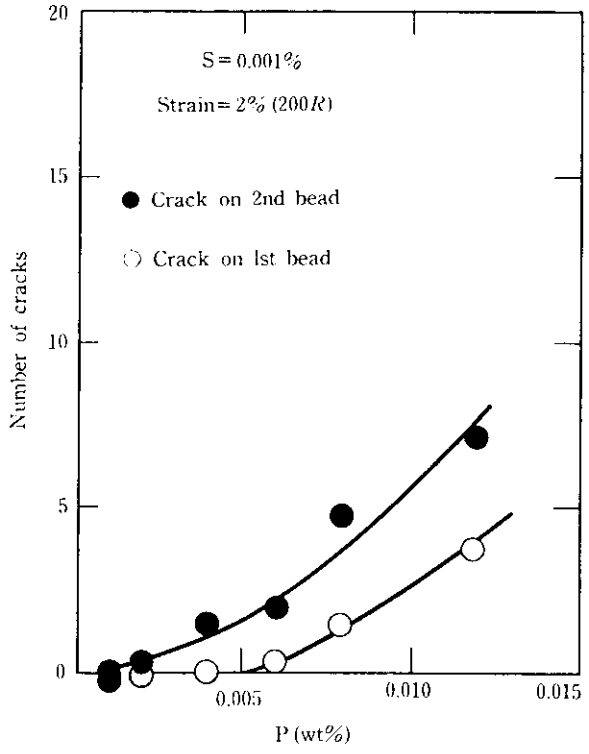

Fig. 2 Influence of P on hot cracking during welding

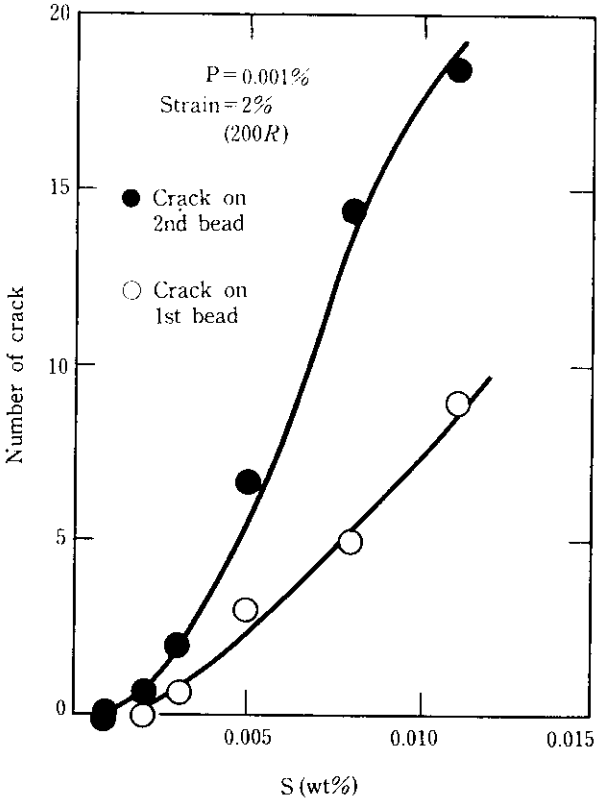

Fig. 3 Influence of S on hot cracking during welding

The results of simultaneous comparison of the effects of P and S are shown in **Fig. 4**. In this figure, the number of cracks generated on the first bead, when 2% strain was applied to specimens in the varestraint test, is stratified, and areas having the same number of cracks are shown with respect to P and S contents. This figure suggests that in order to suppress cracking, it is necessary to strictly control S content. The following relations are valid under such conditions:

$$[\mathrm{P}]\% + 3[\mathrm{S}]\% \leqq 9 \times 10^{-3}\% \quad \text{(Number of cracks} = 0\text{)}$$

$$[\mathrm{P}]\% + 3[\mathrm{S}]\% \leqq 15 \times 10^{-3}\% \quad \text{(Number of cracks} \leqq 4\text{)}$$

These results indicate that S is three times more likely to cause cracking than P.

Further, effects of gaseous impurity elements, O and N, are shown in **Figs. 5** and **6**, respectively. In both cases, cracking susceptibility was determined by the varestraint test, with P and S contents kept at constant values. The O and N contents here are those of the base metal. As O content increases, both reheating hot crack-

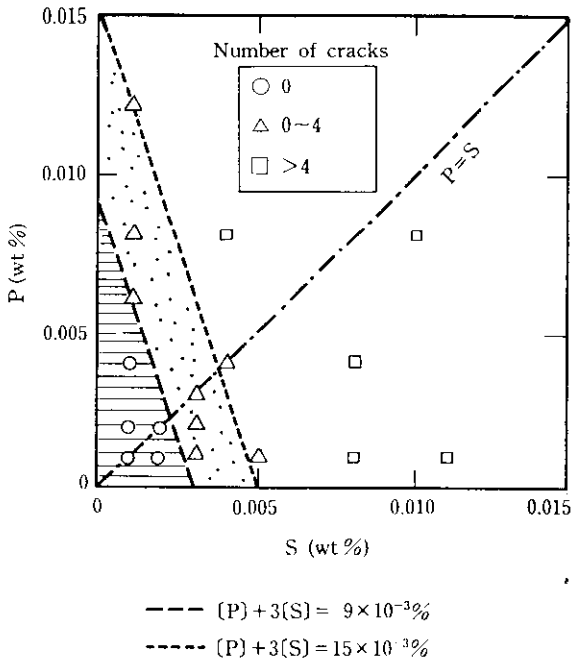

Fig. 4 Simultaneous effect of both P and S on reheating hot cracking during welding

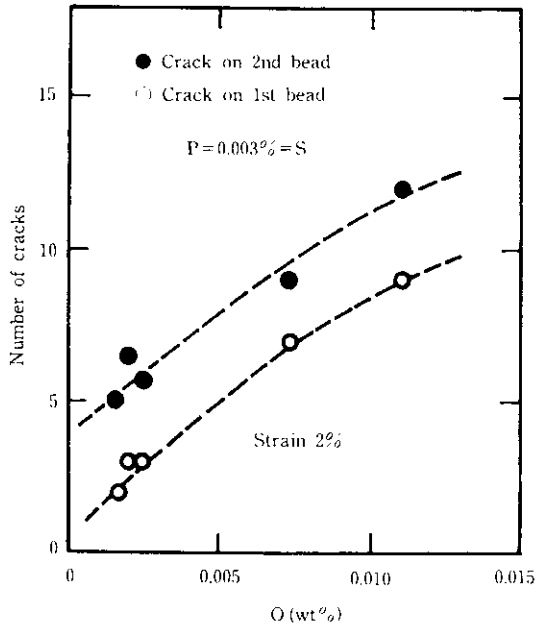

Fig. 5 Influence of oxygen content in mother metal on hot cracking in varestraint weld-crack test

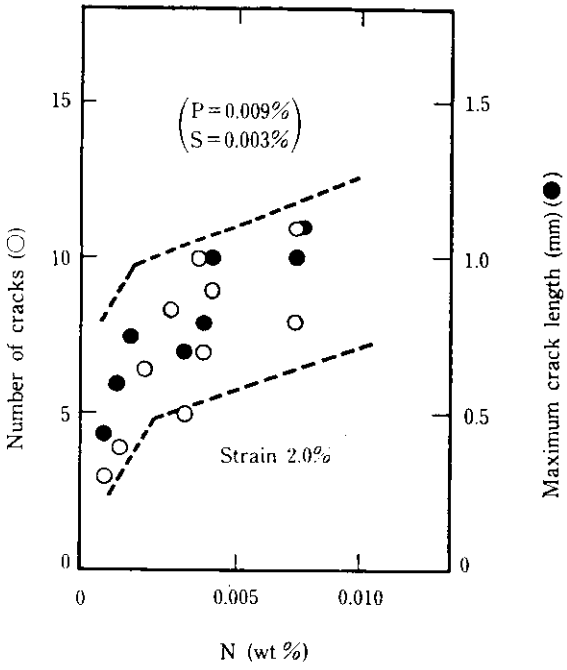

Fig. 6 Influence of nitrogen content in mother metal on reheating hot cracking in varestraint weld-crack test

ing and solidification cracking showed higher frequency of occurrences, thereby suggesting that O is a cause of hot cracking. For N, the number of cracks generated and the total length of cracks in hot cracking when 2% strain was applied are shown. As N content increased, the frequency of generation of hot cracking also increased although this tendency was not so obvious as in the case of O. Since gaseous impurities in base metal promote hot cracking during welding in Fe-36%Ni steel, it is desirable to lower their contents as far as possible, and at the same time, it is necessary to shield against the entry of gaseous impurities from the atmosphere during welding.[7] In connection with the effects of the O content, the weld cracking condition was examined by changing the cleanliness of base metal (that is, the JIS index) within the range of 0.02 to 0.13%. It was confirmed that as the cleanliness deteriorated, crack generation became more probable. This is considered to be related to the fact that as the cleanliness deteriorated, the quantities of soluble oxygen and oxide-based nonmetallic inclusions increased, resulting in increases in O content.

Basic elements of the present steel, when it is assumed that the steel is to be used as membrane material for LNG tanks, are C, Si, Mn, and Ni. An examination was made of the effect on heat cracking during welding of these basic elements together with the effect of Co, which is an accompanying element of Ni, and Al, which is an de-oxidizing element. The results are shown in **Table 3**, which indicates the tested range and crack generation trends of the contents of the basic four elements and of Co and Al together with the results obtained for the above-mentioned micro-impurity elements, P, S, O, N, and cleanliness (d). The upward arrow to the right indicates an increase in crack generating frequency with an increase in the element concerned; the

Table 3 Influence of compositional elements and final cold rolling conditions on reheating hot cracking during varestraint weld-crack test

	Composition (wt%)										d*	Cold rolling		
	C	Si	Mn	Ni	N	Co	Al	P	S	O		CR (%)	Ann. temp. (°C)	GS
Range	0.002 ≀ 0.06	0.10 ≀ 0.20	0.20 ≀ 0.35	35.5 ≀ 38.4	0.003 ≀ 0.010	0 ≀ 1.2	0.003 ≀ 0.02	0.001 ≀ 0.012	0.001 ≀ 0.012	0.002 ≀ 0.012	0.02 ≀ 0.13	40 ≀ 80	850 ≀ 1 100	5 ≀ 10
Crack**	↗	→	→	→	↗	→	→	↗	↗	↗	↗	→	→	→
Note***			→ 0.6~1.0				↗ below 0.005							

* Cleanliness

** Susceptibility to crack:

↗ ; increase with increasing element

→ ; no correlation with element

↘ ; decrease with increasing element

*** Ref. 8)

downward arrow to the right, conversely, indicates a decrease in crack generation frequency with an increase in the element concerned; a horizontal arrow indicates that there is no correlation between crack generating frequency and the element concerned. According to the results, an increase of C promotes cracking, and within the indicated composition range, elements Si, Mn, Ni, Co, and Al have no effect on hot cracking. It must be noted, however that Mn, with a quantity exceeding the range of the present test and amounting to 0.6 to 1.0% had a crack suppressing effect in the Arc-strake solidification cracking test, and that Al within the range of 0.005% or below had a slight crack-promoting effect in the same test.[8] In order to suppress cracking, therefore, it is desirable to decrease the C content as far as possible, but such decreases are limited by the necessity of maintaining low-temperature strength. It thus becomes necessary to consider the control of constituent elements other than C. The greater the inclination of the arrow, the greater degree of effect on cracking; viewed in this manner, it is clear that the effects of P and S are great, followed by O, N, and C.

Since the hot cracking during welding which may occur in this steel is generated in beads which have once melted and solidified, cracking does not seem to be affected by the manufacturing conditions of the base material. Here the effects of the cold rolling ratio, finishing bright annealing temperature, and crystal grain size of this steel sheet have been examined. The results, as shown in Table 3, confirm that these three factors have no practical effect on hot cracking or solidification cracking, as long as they are within the respective ranges of 40 to 80% for rolling ratio, 850 to 1 100°C for an annealing temperature and 5 to 10 for grain size number.

3.1.3 Effects of additive elements

To avoid the generation of hot cracking during welding with this steel, it is particularly desirable to decrease impurity elements such as P, S, O, and N, as mentioned above. However, it is technically difficult and may invite cost increases to reduce these elements, particularly P and S contents, in the actual steelmaking process. From this viewpoint, the criteria for the minimum content of P and S were slightly loosened to P = 0.006% and S = 0.003% (O = 0.0022%; N = 0.0018%), and the effects of some additional elements were examined.

The influence of elements, such as Ti, V, Nb, and Zr, which are considered to have grain-refining and strong S stabilization effect, and elements such as REM and Ca which are considered to have shape-control and S stabilization effect, are shown in **Fig. 7**. All these elements were reported to have some effect in suppressing weld cracking of Fe-36%Ni steel.[9, 10] Regardubg the sample containing no additive elements as a reference, a 0.05% addition of V, from among the four grain-refining elements, was found to be effective to a certain extent, but its effect on hot cracking (H.C.) was minimal. The additive effects of other elements were also minimal, and Zr addition resulted in an increase in susceptibility to solidification cracking. This may be due to cleanliness deterioration brought about by Zr addition. REM addition has almost no effect, and Ca addition gives a slight crack-suppression effect. Further, **Fig. 8** shows the effects of the addition of Cu, W, Mo, Ta, and Hf, which have rarely been given attention previously, in comparison with the reference specimen containing no additive element as in Fig. 7, and with no-additive steel in which P and S contents have been extremely decreased to

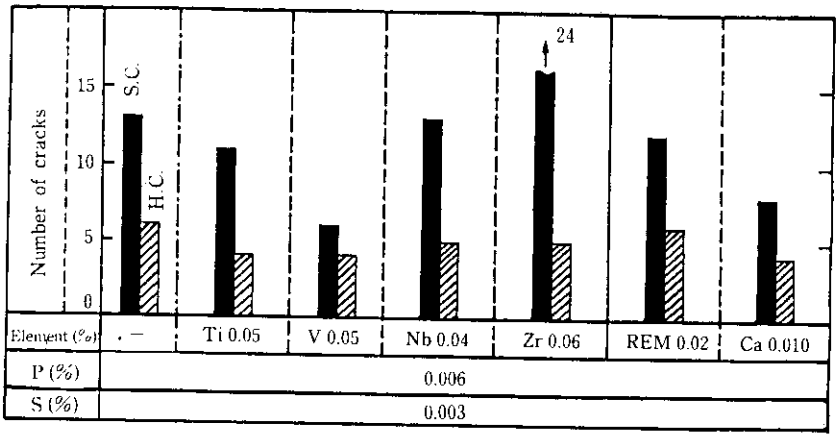

S.C. : Solidification crack on the 2nd bead
H.C.: Reheating crack on the 1st bead
O = 0.0022%
N = 0.0018%

Fig. 7 Influence of alloying elements on hot cracking in welding

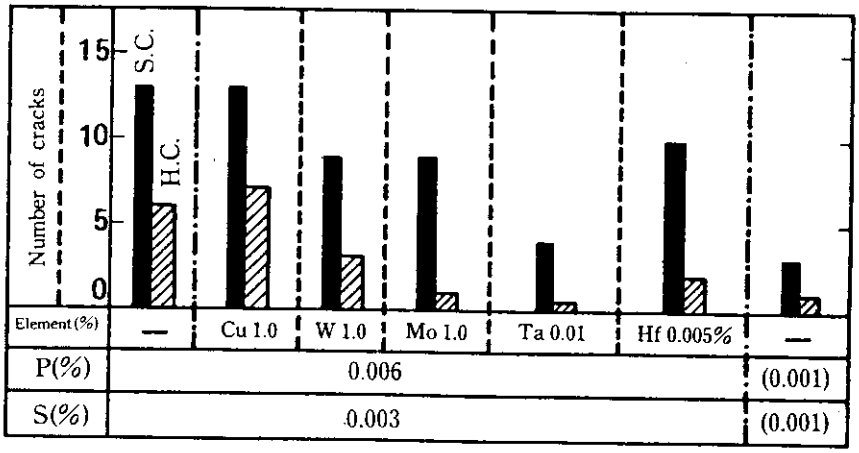

O = 0.0022%
N = 0.0018%

Fig. 8 Influence of Cu, W, Mo, Ta and Hf on hot cracking in welding compared with the specimen containing reduced P and S contents

0.001%. Particularly when attention is focused on hot cracking, Cu addition is totally ineffective, and W addition is only slightly effective. The addition of Mo, Ta or Hf has a considerable effect, and Ta, a remarkable effect. The effect of adding Ta is comparable to that of an extreme decrease in P and S content, and also has a remarkable effect on solidification cracking (S.C.), similar to that of extreme reductions of P and S.

Since the findings regarding the effectiveness of Ta addition are new ones, the effect of Ta addition on weld cracking was examined in more detail. As shown in **Fig. 9**, crack generation was greatly decreased by a Ta addition of up to 0.01% and then decreased gradually with further additions until hot cracking was almost completely suppressed at an addition of about 0.02%.

Photo 4 shows optical micrographs of various specimens selected from those in Fig. 8 and 9 after the varestraint test. Specimens with no additional elements, Zr-added specimens, and Ca-added specimens demonstrated high crack generation rates as shown in Fig. 8, and generation of cracks is clearly visible in the micro-structures. On the other hand, it was observed that specimens with an addition of Mo or Ta rarely showed occurrences of cracks in their micro-structures, and even where cracks occurred, they were minor, being short in length and width. As shown in Photo 2, it is clear that cracks occurred on the moved γ phase grain boundary slightly separated from the solidified crystal boundary. Further, there was no particular difference in crack generation conditions between hot cracking of the first bead, which

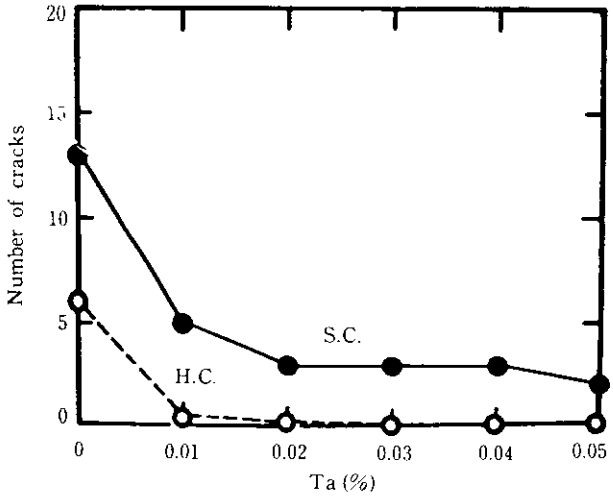

Fig. 9 Relation between number of hot cracks in welding and contents of alloying elements added (S.C. = solidification crack, H.C. = reheating crack)

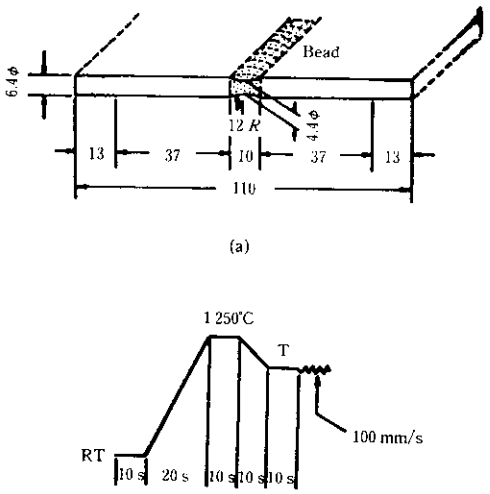

Fig. 10 Shape and size of welded specimen (a) and heat cycle (b) in Gleeble type tension test after quick heating

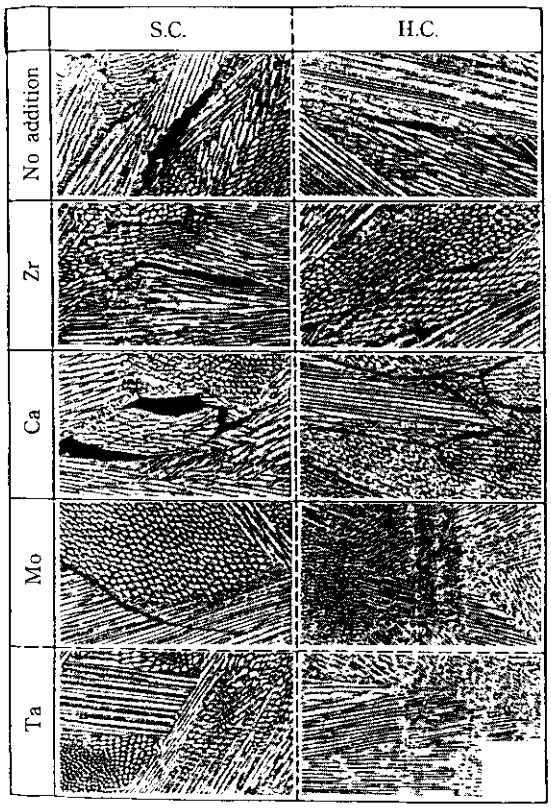

Photo 4 Optical micrographs of solidification cracks (S.C.) and reheating cracks (H.C.) during varestraint test

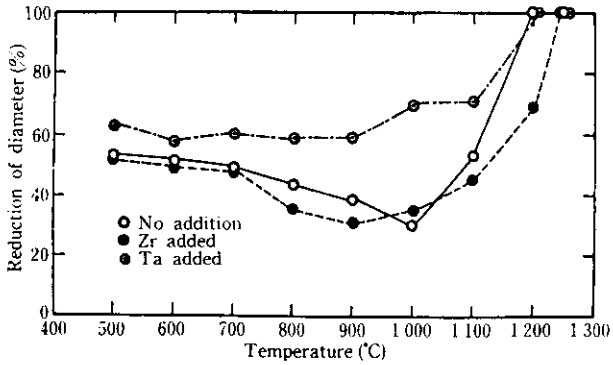

Fig. 11 Change in high temperature ductility obtained from Gleeble type tension test

occurred in the varestraint test, and solidification cracking of the second bead. However, reflecting the difference between the heat treatments, the moving distance of the γ grain boundary is short in the case of solidification cracking, and therefore, the crack generation position tends to be nearer to the solidified crystal boundary.

Examination was made of the causes of the remarkable effect of Ta addition on the suppression of hot cracking during welding. First, the high-temperature ductility of specimens was investigated, using a heat-cycle reproducing apparatus. In this test, a test specimen was made with a weld bead laid at the center of a rod measuring 6.4 mmϕ × 110 mm, and a welding heat cycle test was conducted using a Gleeble testing machine (direct-conduction type rapid heating/cooling tension/compression tester) as shown in **Fig. 10**. The thermal history in the test is shown in the figure. The specimen was rapidly heated to a high temperature (1 250°C), rapidly cooled, and subjected to a tension test at various temperatures and at a velocity of 100 mm/s. **Figure 11** shows the test results. The reduction of diameter both of the reference specimen with no addi-

tional elements and possessing poor weld cracking resistance, and of the Zr-added specimen decreased within the temperature ranges of 900 to 1 100°C, thereby indicating deterioration in high-temperature ductility. By contrast, the Ta-added specimen, which had excellent weld cracking resistance, did not show such a high-temperature embrittlement phenomenon, and its reduction of diameter at 900 and 1 100°C was about twice that of the reference and Zr-added specimens. This may be advantageous in coping with the hot cracking of the present steel, which is liable to occur under constrained stress. This is because the dependence on temperature of the diameter reduction rate when both P and S were greatly decresed to about 0.001%, as shown in Fig. 7, is nearly the same as that of the Ta-added specimen, indicating that the high-temperature ductility and weld cracking susceptibility of the two materials are very similar. The nature of some micromechanism, due to which the reference specimen easily cracked but the Ta-added specimen and the specimen with decreased P and S contents were resistent to cracking, was subjected to micro-and macro-analyzer analyses. No clarification has been obtainable, and this constitutes a future task. Formation of fine precipitates in a shape of dotted-line along the crack-developing moving grain boundary has yet been confirmed by extraction replica electron micrography of the fracture surface,[11] and analysis and identification of the precipitates and their relation to the cracking phenomenon will be undertaken.

3.2 Anti-rust Property, Physical and Mechanical Properties and Formability

3.2.1 Anti-rust property

Another problem that ranks with weld cracking of Invar-type Fe-36%Ni steel is anti-rust property. In LNG tanks, the steel will not corrode once cooled, but it is a concern that rust may be caused by dewing during tank use, which occurs when the liquid level in the LNG tank drops greatly. Further, the construction process from the carrying-in of the material to the completion and cooling-down of the tank may involve more difficult rust problems. Conceivable countermeasures are air-conditioning of the factory on the fabricator side, and surface treatment[4] or composition control[12] on the supplier side. In order to study the improvement of anti-rust property by the addition of micro-quantity elements, a salt spray test, as stipulated by JIS, and an atmospheric exposure test were conducted, with the results shown here. The relation between the rusting ratio and spraying time in the salt spray test is shown in **Fig. 12**. In this test ordinary Fe-36%Ni steel developed rust on almost the entire surface of the specimen in about 100 min, while the same steel with the addition of Cr, Ti, or Co, in comparison, showed a greatly retarded rusting speed. The

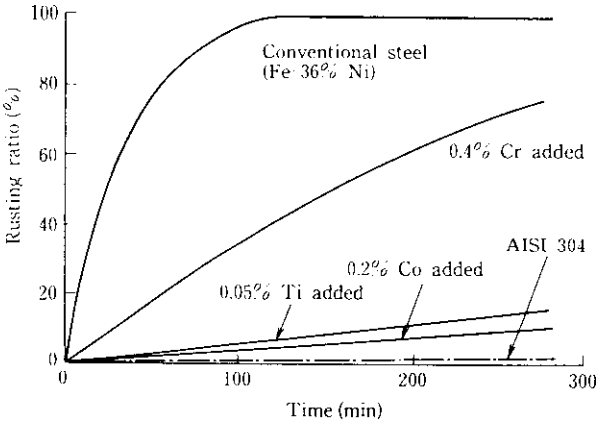

Fig. 12 Results of salt spray test of Fe-36%Ni specimens with and without alloying elements

same tendency was also observed in the atmospheric exposure test, indicating that additions of small amounts of these elements will considerably improve the anti-rust property. It is important to note that these elements can be added without causing deterioration of the low thermal expansivity which is a special feature of the present steel. Ti addition, however, is not desirable, because it increases O content, deteriorates cleanliness, and is harmful to weld cracking resistance. According to the results of the stress corrosion cracking test, Co content of 1% or more will increase crack sensitivity. Therefore, it is desirable to restrict Co content to below 1% in view of stress corrosion cracking susceptibility, although a certain content of Co is desirable from the viewpoint of anti-rust property and reductions in cost related to the use of ferro-Ni as a raw material.

3.2.2 Physical and mechanical properties

As a result of an examination of resistance against hot cracking during welding and the anti-rust (corrosion) property which posed problems in Invar-type Fe-36%Ni steel, it was found that these characteristics can be improved by impurity-element content control and addition of micro-quantity alloy elements. On the basis of the present results, the composition design shown in **Table 4** was formulated, and a new Fe-36%Ni steel (KLN 36) was developed.[12-14] In this steel, to improve weld cracking resistance, P, S, O, and N were decreased, and Ta was added. To improve the anti-rust property, small amounts of Cr and Co were added. Due to Ta addition, there was no need for extreme reductions in P and S which would have invited cost increases.

Physical properties of the newly developed steel are shown in **Table 5**. Very small thermal expansivity was obtained at below room temperature. The average linear thermal expansion coefficient within the temperature range from −185 to 20°C of the typical sample shown in Table 4 was sufficiently small as 1.4×10^{-6}/°C, and the Curie point was measured as 250°C.

Table 4 Chemical composition of newly developed Fe-36%Ni steel "KLN 36"

(wt%)

	C	Si	Mn	P	S	Ni	N	O	Al
Composition range	≦0.04	≦0.3	≦0.5	≦0.015	≦0.005	35.5-36.0	≦0.003	≦0.003	≦0.05
Typical example	0.03	0.2	0.35	0.005	0.002	35.9	0.0020	0.0018	0.03

Others: Ta, Cr or Co addition (Ex. Ta=0.02, Cr=0.25, Co=0.22).
ASTM Standard: C=0.10, Mn=0.50, P=0.025, S=0.025, Si=0.40, Ni=35.5-36.5, Cr=0.50, Mo=0.50, Co=0.50

Table 5 Physical properties of newly developed Fe-36%Ni steel "KLN 36"

No.	Properties	Temperature	Value
1	Thermal expansivity ($°C^{-1}$)	−185~20°C	1.4×10^{-6}
2	Young's modulus (kgf/mm^2)	20°C	14 700
3	Specific heat (cal/g·°C)	〃	0.10
4	Electric resistivity ($\mu\cdot\Omega$·cm)	〃	6.8
5	Density (g/cm^3)	〃	8.11
6	Thermal conductivity (cal/cm·°C)	〃	0.030
7	Curie point (°C)	—	250 (ferromagnetic)

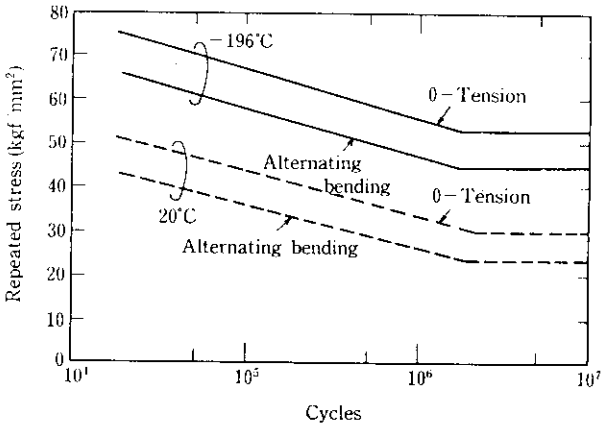

Fig. 13 Fatigue test results of newly developed Fe-36%Ni steel "KLN 36" by tension and bending fatigue

The ordinary service temperature of the present steel for LNG-carrier and on-shore LNG tank is about −162°C, but **Table 6** shows mechanical properties (tensile strength, ductility, toughness, and notch characteristics) at the temperature of liquefied nitrogen (−196°C), which is slightly lower than this temperature (−162°C), and also at room temperature. As can be seen from this Table, the newly developed steel has sufficient strength, ductility, and toughness at both room and low temperatures. To determine its notch sensitivity, tensile tests using a specimen with a 0.2 mm$R$ V-notch and a flat specimen were conducted at room and low temperatures. According to the test result, the notch sensitivity of the steel is considered sufficiently small, as shown in Table 4. Results of the alternating flat-plane bending fatigue test and partial single-amplitude 0-tension fatigue test are shown in **Fig. 13**. The tests were conducted at room temperature and −196°C using a smooth specimen. The ratio of the fatigue limit to stationary tensile strength was within the range of 0.5 to 0.6 in all cases, figures not much different from those of austenitic stainless steel and aluminum alloy.

3.2.3 Formability and application to model tank

When constructing an LNG membrane tank, excellent formability of materials is required. As can be

Table 6 Mechanical property of newly developed Fe-36%Ni steel "KLN 36" together with notch toughness

	Mechanical property					Notch toughness		
Temp. (°C)	0.2% Proof stress $\sigma_{0.2}$ (kgf/mm^2)	Tensile stress σ_u (kgf/mm^2)	Elongation λ (%)	Hardness (HV)	Charpy value ($kgf\cdot m/cm^2$)	$\sigma_{0.2,n}/\sigma_{0.2,f}$	$\sigma_{u,n}/\sigma_{u,f}$	λ_n/λ_f
20	30	30	35	135	33	1.07	1.06	0.95
−196	63	90	37	—	24	1.12	1.08	0.93

n: notch specimen
f: flat specimen

Photo 5 LNG model tank built using newly developed Fe-36%Ni Steel "KLN 36"

easily seen from the results of the present tests for ultimate tensile elongation, hardness, and toughness, the formability of the newly developed steel is intrinsically excellent. In fact, in a bending test at room temperature, it was possible to bend a specimen with a sheet thickness of 0.5 to 1.5 mm without regard to angle from the rolling direction. When a forming machine was used to give tong work of 90° and 150° on a base-material sheet of 0.5 mm$t$ × 50 mm$W$ × 5 000 mm$L$, it was found that bendability was excellent; no cracking was observed, and burr condition and external appearance were satisfactory. There was no problem in forming a groove of 3 mm in depth and 4 mm in width from the same sheet. Further, when specimens with a width of about 500 mm and thicknesses of 0.7 and 1.0 mm were subjected to both-flange bending (2 000 mm in length) and single-flange bending (7 000 mm in length), excellent formability was observed in warping, bending, rectangularity, surface flaws, and flange-height deviation.

Shape and dimensional accuracy of these long-sized sheets must be as good as possible, and the newly developed steel satisfies the dimensional tolerances, for instance, of the membrane tank of the GT type LNG carrier when it was given process treatment such as Sendzimir-mill rolling, bright annealing, and high-tension skinpass rolling.[15] The new steel manufactured through actual processes, which had undergone the above-mentioned forming tests, was used to construct a model membrane tank of the GT-type LNG carrier (**Photo 5**). The properties of the newly-developed steel were found to be excellent when compared with those of conventional steel; the new steel developed no weld cracking and passed the prescribed leak test successfully. From these results, the newly-developed steel was considered to have overcome the defects associated with conventional steel and be practically applicable to LNG tanks.

4 Conclusions

Effects of composition balance on hot cracking during welding and anti-rust property, which have posed problems with Invar-type Fe-36%Ni steel, have been studied, and on the basis of the results of the examination, a new Invar alloy KLN36 has been developed. The experimental results are summarized below.

(1) Impurity elements such as P, S, O, N and a basic element C contribute greatly to hot cracking. In order to improve the crack resistance of Invar-type alloy steel, it is necessary to decrease contents of these elements. By satisfying the condition of "[P]% + 3[S]% $\leqq 9 \times 10^{-3}$%," it has become possible to greatly reduce cracking.

(2) Micro-amount addition of alloy elements such as Mo, Ta, and Hf is also effective against hot cracking during welding, and in particular, the effect of Ta is remarkable. This fact has been confirmed by the high-temperature ductility behavior of the alloy steel in the Gleeble test. Addition of V, Nb, Ti, Zr and Ca is ineffective.

(3) It has been found that micro-amount addition of Cr, Co, and Ti is effective in improving the anti-rust property of the steel. Ti addition, however, is not desirable, as it is necessary to maintain the cleanliness of the steel. The addition of Cr and Co is preferred. Addition of some amounts of these elements will not degrade the low thermal expansivity which is an important feature of the steel.

(4) As a result, KLN36, a steel with decreased contents of impurity elements such as P, O, S, and N and the addition of Ta, Cr, and Co, has been developed as a new Invar alloy. It features excellent resistance to hot cracking during welding and is excellent in anti-rust property. Physical and mechanical properties of KLN36 at room temperature and extreme low temperature (−196°C) have been indicated.

(5) A forming test involving actual processing of KLN36 products was conducted, and satisfactory results were obtained. After the forming test, these

products were used to construct a model GT-type LNG carrier tank, with satisfactory results in terms both of the absence of weld cracking and of leak-proofing as confirmed by a leak test.

Finally, the authors would like to express their deep appreciation to Prof. F. Matsuda and Dr. Hiroshi Nakagawa, Welding Research Institute of Osaka University, and Messrs. S. Minehisa and N. Sakabata, Hitachi Zosen Corp. (Research Laboratory), for the valuable advice they gave in the course of the weld cracking examination, and to Messrs. Y. Katada, K. Hayakawa, and S. Dazai, also of the same company (Hiroshima Factory) for giving the authors the opportunity to participate in the forming test and model tank construction.

References

1) M. A. Hunter: "Metals Handbook," **1**(1961), 816, [ASM]
2) F. Duffaut: "LNG Workshop," Paris (1983)
3) F. Matsuda, H. Nakagawa, S. Minehisa, N. Sakabata, A. Ejima, and K. Nohara: *Tetsu-to-Hagané*, **69**(1983)13, S1160
4) S. Maruhashi, K. Hoshino, S. Osaki, T. Ideguchi, I. Uchida, and T. Igita: *Tetsu-to-Hagané*, **67**(1981)12, S1391
5) H. Nakagawa, F. Matsuda, A. Nagai, and N. Sakabata: Trans. JWRI, **2**(1980)1, 197
6) F. Matsuda, H. Nakagawa, S. Minehisa, N. Sakabata, A. Ejima, and K. Nohara: *Tetsu-to-Hagané*, **70**(1984)5, S648
7) H. Nakagawa, F. Matsuda, S. Minehisa, N. Sakabata, A. Ejima, and K. Nohara: *Trans. JWRI*, **13**(1984)2, 69
8) H. Kanesashi and M. Inoue: *Tetsu-to-Hagané*, **65**(1979)4, S476
9) Creusot Loire S. A.: Jpn. Kokoku 46-26220
10) Nippon Yakin Kogyo Co. Ltd.: Jpn. Kokai 53-83921
11) F. Matsuda, H. Nakagawa, S. Minehisa, N. Sakabata, A. Ejima, and K. Nohara: submitted to Tetsu-to-Hagané
12) Kawasaki Steel Corp.: Jpn. Kokai 56-044749
13) Kawasaki Steel Corp.: Jpn. Kokai 57-207154
14) Kawasaki Steel Corp.: Report submitted to BV, public communication
15) Gaz Transport: Ext. Doc. No. 338A (1979) and No. 338C (1982)